

Influence of electrolyte temperature on spectral properties of porous silicon microcavity

Hongyan Zhang (张红燕)¹, Rongxia Liu (刘荣霞)¹, Xiaoyi Lü (吕小毅)², and Zhenhong Jia (贾振红)^{2*}

¹School of Physical Science and Technology, Xinjiang University, Urumqi 830046, China

²Colleges of Information Science and Engineering, Xinjiang University, Urumqi 830046, China

*Corresponding author: jzh@xju.edu.cn

Received September 27, 2013; accepted October 18, 2013; posted online February 26, 2014

A porous silicon microcavity (PSM) is highly sensitive for sensing applications due to its high surface area and a narrow resonance peak. In this letter, we fabricated the PSM by alternate current density from a low value to a high value during double-tank electrochemical anodization at different electrolyte temperatures. Results show that with the increase of the electrolyte temperature, the rate of the PS etching becomes faster and the refractive index of the PS layer becomes smaller. The thickness of the PS increases faster than the decrease of the refractive index of the PS.

OCIS codes: 240.6695, 160.4670, 160.3900, 300.6450.

doi: 10.3788/COL201412.S12402.

Nanomaterials have been a focus of nanoscience and nanotechnology, which are attracting tremendous interests, investments and efforts in research and development around world. Nanoporous materials as a subset of nanostructured materials possess a large specific area structural and bulk properties. Especially, porous silicon (PS) is one of most promising nanostructured materials with the large internal surface area (up to 800 m²/g)^[1]. It allows immobilization of more probe molecules, which increases the possibility of capturing low-concentration target molecules in solution. The absorption of substance into the pores modifies the electrical and optical properties of PS, such as electrical conductivity, photoluminescence (PL) and reflectance spectrum^[2-4]. These properties of PS have lead to wide applications in chemical sensing, organic vapor sensing and biological sensing. Furthermore, PS is an ideal material for optoelectronic devices, such as light emitting diodes (LEDs) and waveguides^[5,6].

In recent years, the study of interaction between optical and electric states in optical microcavities has become an important research area, resulting in key technological advancements such as high-efficiency semiconductor laser and label-free optical biosensor. PS has great potential for microcavity fabrication and development, since the refractive index value of the PS can be tuned over a wide range. In this paper, we fabricated a PSM using an alternate-current density through electrochemical anodization. The optical characteristic of the PSM structure is of a highly reflective stop band with a narrow resonance peak of transmittance approximately in the center of this stop band. However, fabrication of PSM using traditional electrochemical anodization is limited by several technical problems, one of which is how the temperature affects the refractive index value and thickness when a multilayer system is formed. This is of great importance for the resonance peak of the PSM in the measured reflectivity spectrum. For that purpose, we fabricated a PSM by controlling current density alternately switched from a low value to a high

value during the electrochemical formation process, which results in alternate low- and high-porosity layers. We got different measured resonance peaks of PSM in reflectivity spectra at different electrolyte temperature.

The PSMs were fabricated with highly doped p-type (100) Si with a resistivity of 0.01 – 0.02 Ωcm and 420 + 15-μm thickness. The substrates were cut into squares and cleaned with a solution of acetone, alcohol, and deionized water. Then the PSMs were obtained by electrochemical anodization in mixed solution of 49% aqueous hydrofluoric acid and ethanol (1:1 by volume). The structure of the PSM was fabricated following the $(n_H n_L)^7 n_H n_{Lc} n_H (n_L n_H)^7$ sequence. In order to get different refractive index layer, the silicon wafer was anodized using a computer program (Labview) to alternate the anodization current for difference etching times in electrochemical anodization process. As shown in Fig.1, the two DBRs were fabricated using a current density alternating between 20 mA/cm² for 4.1s (n_H layers) and 80 mA/cm² for 6.1 s (n_L layers). The optical cavity layer (n_{Lc} layer) was formed at a current density of 80 mA/cm² for 15.3 s with a 3-s pause after each

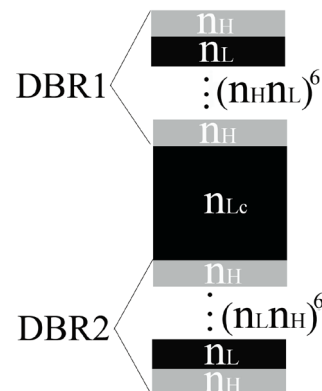


Fig. 1. Diagram of the PSM structure.

layer formation. In the teflon electrochemical etch cell, the copper was the cathode and the saturated salt water was an anode as a counter electrode. In this teflon electrochemical etch cell, silicon wafer directly contacted with saturated salt water^[7], which was helpful for electrolyte temperature control. In this experiment, in order to study the influence of the electrolyte temperature on the resonance peak of PSM in reflectivity spectra, the electrolyte temperature was maintained at 3 °C, 6 °C and 9 °C, separately.

Fig. 2 shows a cross-sectional image of the PSM fabricated at 9°C following the $(n_H n_L)^7 n_H n_{Lc} n_H (n_L n_H)^7$ sequence. The thickness of the PSM on the silicon wafer was approximately 7.21 μm and a multilayered stack was clearly identified. It can be clearly seen that all the constituted layers in the PSM were preserved after totally completing the entire electrochemical anodization process.

Fig. 3 shows the surface images of the PSM produced by electrochemical anodization at different electrolyte temperature. The pore distribution is random and the porosity is increased with the electrolyte temperature. Higher porosity corresponds to lower refractive index.

Fig. 4 shows the reflectance spectra of the PSM fabricated at different electrolyte temperature following the same $(n_H n_L)^7 n_H n_{Lc} n_H (n_L n_H)^7$ sequence. The reflectance resonant peak at 1163 nm, 1341 nm and 1459 nm corresponds to electrolyte temperature at 3 °C, 6 °C and 9 °C, respectively. In Fig. 3, we can see that refractive index become lower with the electrolyte temperature increasing. From the optical point of view, for the reflectance spectrum of multilayered sample such as PSM structure, the reflectance maximum appears at Bragg wavelengths (λ_{Bragg}) satisfying the relation as:m $\lambda_{\text{Bragg}}/2 = n_L d_L + n_H d_H$. From Fig. 4, we can deduce that

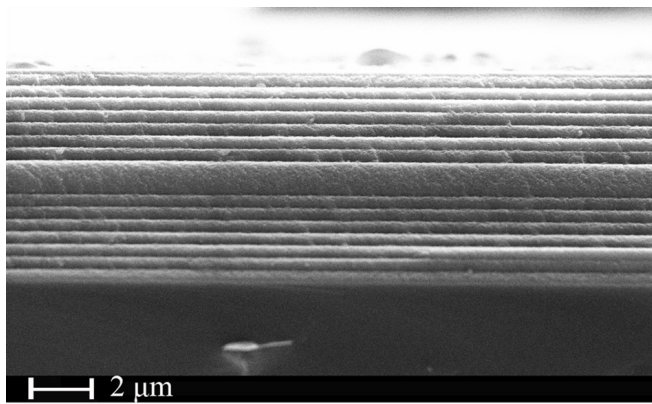


Fig. 2. Cross-sectional image of the PSM following the $(n_H n_L)^7 n_H n_{Lc} n_H (n_L n_H)^7$ sequence.

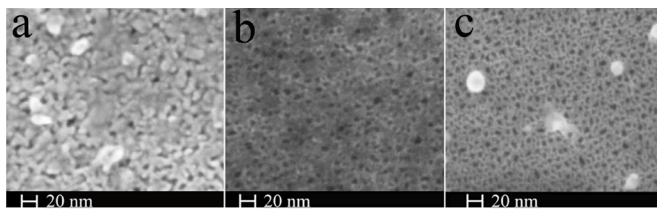


Fig. 3. Top views of surface images of the PSM fabricated at (a) 3 °C, (b) 6 °C, and (c) 9 °C.

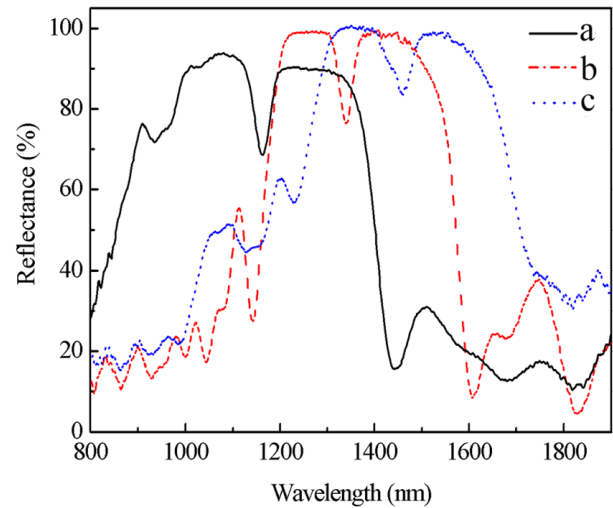


Fig. 4. Reflectance spectra of PSM fabricated at (a) 3 °C, (b) 6 °C, and (c) 9 °C.

with the electrolyte temperature increasing, the refractive index of PS layer becomes lower and the reflectance resonance peak becomes longer. According to the Fabry–Perot relation, the thickness of the PS increases faster than the decrease of the refractive index of the PS.

In this paper, we fabricated PSMs by controlling current density alternately switched between a low value and a high value during the double tank electrochemical anodization and studied the influence of electrolyte temperature on spectral properties of porous silicon microcavity. Results show that with the increase of electrolyte temperature, the rate of the PS etching becomes faster and the refractive index of the PS layer goes lower. The thickness of PS increases with the temperature increasing, and the refractive index decreases at the same time. These two factors combined together result in that reflectance spectrum of PSM moves to longer wavelength. This research is helpful for the fabrication of the PSM and has great potential for biosensors based on optoelectronic devices.

This work was supported by the National Science Foundation of China (No. 60968002 and 61265009), Research Foundation for the Doctoral Program of Chinese Universities (No. 20116501110003), and Xinjiang Science and Technology Project (No. 201291109 and 2012211B01).

References

1. M. Hiraoui, L. Haji, M. Guendouz, N. Lorrain, A. Moadhen, and M. Oueslati, *Biosens Bioelectron.* **36**, 1 (2012).
2. H. Kim, Y. Kim, K. Lee, and S. Park, *Sens. Actuators B.* **155**, 2 (2011).
3. B. Benyahia, L. Guerbous, N. Gabouze, and Br. Mahmoudi, *Thin Solid Films* **540**, 1 (2013).
4. M. Hiraouia, M. Guendouz, N. Lorrain, A. Moadhen, L. Haji, and M. Oueslati, *Mater. Chem. Physl.* **128**, 1 (2011).
5. B. Das and S.P. McGinnis, *Semicond. Sci. Technol.* **14**, 11 (1999).
6. G. Barillaro, F. Pieri, and U. Mastromatteo, *Opt. Mater.* **17**, 1 (2001).
7. H. Zhang, Z. Jia, X. Lü, J. Zhou, L. Chen, R. Liu, and J. Ma, *Biosens Bioelectron.* **44**, 15 (2013).